

Phylogenetic comparative methods for studying adaptation: the adaptation-inertia framework

Jason Pienaar^{1, ID}, Krzysztof Bartoszek^{2, ID}, Bayu Brahmantio^{2, ID}, Janna L. Fierst¹, Jesualdo A. Fuentes-González¹, Thomas F. Hansen³, Woodrow Hao C. Kiang², Bjørn T. Kopperud^{4,5}, Kjetil L. Voje^{6, ID}

¹The Institute of Environment and the Biomolecular Sciences Institute, Florida International University, Miami, United States

²Department of Computer and Information Science, Linköping University, Linköping, Sweden

³Center for Evolutionary and Ecological Synthesis, Department of Biology, University of Oslo, Oslo, Norway

⁴Department of Earth and Environmental Sciences, Paleontology and Geobiology, Ludwig-Maximilians-Universität München, Munich, Germany

⁵GeoBio-Center, Ludwig-Maximilians-Universität München, Munich, Germany

⁶Natural History Museum, University of Oslo, Oslo, Norway

Handling Editor: Alejandro Gonzalez-Voyer, Associate Editor: Patrick Rohner

Corresponding author: Jason Pienaar, Institute of Environment & Biomolecular Sciences Institute, Florida International University, 11200 SW 8th Street, Miami, FL 33199, United States. Email: jpienaar@fiu.edu

Abstract

Phylogenetic comparative methods are a major tool for evaluating macroevolutionary hypotheses. Methods based on the mean-reverting stochastic Ornstein–Uhlenbeck process allow for modelling adaptation on a phenotypic adaptive landscape that itself evolves and where fitness peaks depend on measured characteristics of the external environment and/or other organismal traits. Here, we give an overview of the conceptual framework for the many implementations of these methods and discuss how we might interpret estimated parameters. We emphasize that the ability to model a changing adaptive landscape sets these methods apart from other approaches and discuss why this aspect captures long-term trait evolution more realistically. Recent multivariate extensions of these methods provide a powerful framework for testing evolutionary hypotheses but are also more complicated to use and interpret. We provide some guidance on their usage and put recent literature on the topic in biological rather than mathematical terms. We further show how these methods provide a starting point for modelling reciprocal selection (i.e., coevolution) between interacting lineages. We then briefly review some critiques of the methodologies. Finally, we provide some ideas for future developments that we think will be useful to evolutionary biologists.

Keywords: Adaptation, Phylogenetic Comparative Methods, Macroevolution, Adaptive Landscape, Phylogenetic Inertia, Ornstein–Uhlenbeck Process

Introduction

“Response to selection pressure is not instantaneous, and inertia, in the sense of lag in following a shifting optimum, is an important element in evolution”—Simpson (1944) pp 179.

The modern synthesis of evolutionary theory has long wrestled with Dobzhansky's (1937) and many subsequent biologists' supposition that microevolutionary forces scale up to explain macroevolutionary patterns. Although the origins of new life forms, transitional changes, and rates of evolution have traditionally been the focus of evolutionary biology, explanations for the persistent lack of change in traits over long time periods—the “paradox of stasis”—remains a significant challenge (Bradshaw, 1991; Eldredge & Gould, 1972; Futuyma, 2010; Hansen, 2012; Hansen & Houle, 2004; Williams, 1992), especially given the high evolvability observed in almost all quantitative traits where evolvability has been studied (Hansen & Pélabon, 2021).

A promising approach to understanding long-term phenotypic evolution stems from Simpson's (1944) pheno-

typic adaptive-landscape metaphor, inspired by Wright's (1931) adaptive landscape for genotypes, except that it envisions a dynamic topographical landscape of adaptive zones for phenotypes rather than genotypes. The topographical shape of Simpson's landscape at any given time is thus defined by where current trait values are in relation to the fitness peaks of the adaptive zones and how strong selection towards those peaks is. Although early models like Lande's (1976) influential model of stabilizing selection and genetic drift describe phenotypic evolution on such a landscape over generational timescales, they often fail to capture the phylogenetic correlations and degree of cross-species variation observed in macroevolution. This is because Lande's selection-drift model is built for a static adaptive landscape, that over macroevolutionary timescales, nearly always results in a near-instantaneous approach to the optimum. This implies that there will be no phylogenetic correlations, no lingering influence of past environments, and therefore, that phylogenetic comparative methods are simply unnecessary (Hansen & Martins, 1996). Phylogenetic signal, however, is ubiquitous across millions of years (Uyeda et al., 2011). Simpson (1944,

Received October 30, 2023; revised July 24, 2025; accepted August 27, 2025

© The Author(s) 2025. Published by Oxford University Press on behalf of the European Society of Evolutionary Biology. All rights reserved. For commercial re-use, please contact reprints@oup.com for reprints and translation rights for reprints. All other permissions can be obtained through our RightsLink service via the Permissions link on the article page on our site—for further information please contact journals.permissions@oup.com

1953) and others (e.g., Arnold, 2023; Arnold et al., 2001; Calsbeek et al., 2012) have argued that the adaptive landscape is a dynamic entity that itself evolves over macroevolutionary time scales and that it is this dynamic aspect of the landscape that potentially generates a lag between species trait values and their shifting optima, observed cross-species variation levels, and phylogenetic correlations.

Phylogenetic comparative analyses across groups of related species have long been used to test macroevolutionary hypotheses (Brooks & McLennan, 1991; Rensch, 1959; Ridley, 1983). These methods use phylogenetic relatedness to statistically account for the non-independence of trait observations among related species. It is less appreciated, however, that how much traits are dependent (or are free to vary) relies on both phylogenetic relatedness as well as the mode of evolution unfolding in the phylogeny. Felsenstein (1985) lucidly showed this model dependence when he developed the independent-contrasts algorithm, which assumes trait evolution follows a multivariate Brownian motion, meaning evolutionary changes across the phylogeny are proportional to shared ancestral time. When accounting for the relatedness of species in statistical analyses once the model of evolution unfolding on the phylogeny has been accounted for, methods like generalized least squares (Grafen, 1989; Martins & Hansen, 1997; Rohlf, 2001), likelihood (Lynch, 1991), or Bayesian approaches (Hadfield, 2010; Uyeda & Harmon, 2014) can estimate model parameters by specifying the covariance among residuals. To address the dynamic adaptive landscape issue, the “adaptation-inertia” phylogenetic comparative analysis framework inspired by Hansen’s (1997) work uses the stochastic, mean-reverting Ornstein–Uhlenbeck process to model trait evolution. This framework explicitly accounts for how trait values move towards specific adaptive optima, which can change with environmental variables. The approach builds upon a rich history of statistically rigorous, evolutionary-model based phylogenetic comparative methods developed since the 1980s (Armbuster, 1988; Cheverud et al., 1985; Felsenstein, 1985, 1988; Pagel & Harvey, 1988). The Ornstein–Uhlenbeck process, as described below, allows for distinguishing between general phylogenetic signal and phylogenetic inertia by controlling only for the latter defined as a lag in adaptation to evolving fitness peaks. This distinction becomes particularly important when traits adapt to fitness peaks that themselves are phylogenetically structured (as would be the case when organisms, for example, track their ancestral niches) as this will show up as general phylogenetic signal in the traits, and it could potentially be a mistake to attempt to correct for it, which unfortunately is still common practice, especially when the traits do not lag behind their fitness peaks (Hansen, 2014; Hansen & Orzack, 2005; Labra et al., 2009; Revell, 2010). Importantly, this framework also allows for fitness peaks to remain stationary over long time periods (or indefinitely) and for evolution to be bounded around such fitness peaks, thereby providing one possible explanation for stasis—long term stabilizing selection. The suite of methods in the “adaptation-inertia” framework can now model various types of traits, continuously varying or categorical, and offers a robust toolset for analyzing macroevolution and adaptation.

In this review, we discuss the rationale and parameter interpretation of the adaptation-inertia framework, its relationship to quantitative genetic models, detail its various extensions, and explore how its multivariate methods can illuminate trait

interactions and coevolutionary processes by means of an example. It is our hope that this review will serve as a useful guide to this rich and rapidly expanding modelling framework for both new and experienced users.

The adaptation-inertia modelling framework

The adaptation-inertia framework models how species’ trait values track shifting adaptive fitness peaks, influenced by environmental factors (Hansen, 1997). It aims to determine if species in different niches have systematically distinct adaptive peaks. To this end, Hansen (1997) proposed estimating a “primary optimum,” representing the average trait state for species evolving in a specific adaptive zone over long periods. Individual species have local trait optima that vary around this primary optimum, averaging out secondary evolutionary influences. For example, fig wasps pollinating monoecious *Ficus* species have on average, longer ovipositors than those pollinating dioecious *Ficus* species (Nefdt & Compton, 1996), reflecting the bimodal style lengths they must navigate to successfully reproduce. Male monoecious fig flowers, on average, have longer styles than the male flowers of dioecious figs, and fig-species-specific fig wasp mothers must insert their ovipositors through these styles in either case to successfully lay an egg and provide their larvae with nutrition through galling the uni-ovulate flowers. Differences in these primary optima indicate the systematic influence of distinct primary niches (like the bimodal style lengths associated with monoecy vs. dioecy) on adaptive peak positions. To assess the importance of adaptation to a niche, the framework examines how different these primary optima are and how quickly species adapt to them, while also accounting for unmeasured factors influencing local adaptive-peak changes. A simple model that allows for incorporating all these requirements is the Ornstein–Uhlenbeck process. It consists of a deterministic part describing the approach to the primary optimum and a stochastic part representing changes in adaptive peaks due to a combination of numerous unknown and unmeasured secondary selective forces as well as other stochastic processes such as genetic drift. Mathematically, the Ornstein–Uhlenbeck process is described by the stochastic differential equation:

$$dy = -\alpha (y - \theta) dt + \sigma dW, \quad (1)$$

where dy is the change in the adaptive peak over an infinitesimal time interval dt , y is the position of the adaptive peak, θ is the primary optimum, α (≥ 0) determines the rate of adaptation towards the primary optimum, dW is short-hand for independent normally distributed stochastic changes with mean zero and unit variance over a unit of time (white noise), and σ is the instantaneous standard deviation of these changes (i.e., W is a Brownian motion process). The model stipulates that the rate of adaptation to the primary optimum increases linearly with distance from that optimum. To represent alternative niches, we can extend the basic model by allowing the primary optimum to be a function of one or more indicators, x_i , that represent niches or environmental states. Hence, we write $\theta = \theta(x_i)$ in the model. Using a method developed in Hansen & Martins (1996), Hansen (1997) derived the joint distribution of species trait values when this process unfolds on a phylogeny. This assumes that the states of the niche predictor variables, x_i , are known on the phylogeny. The joint distribution is multivariate normal with a predicted mean for

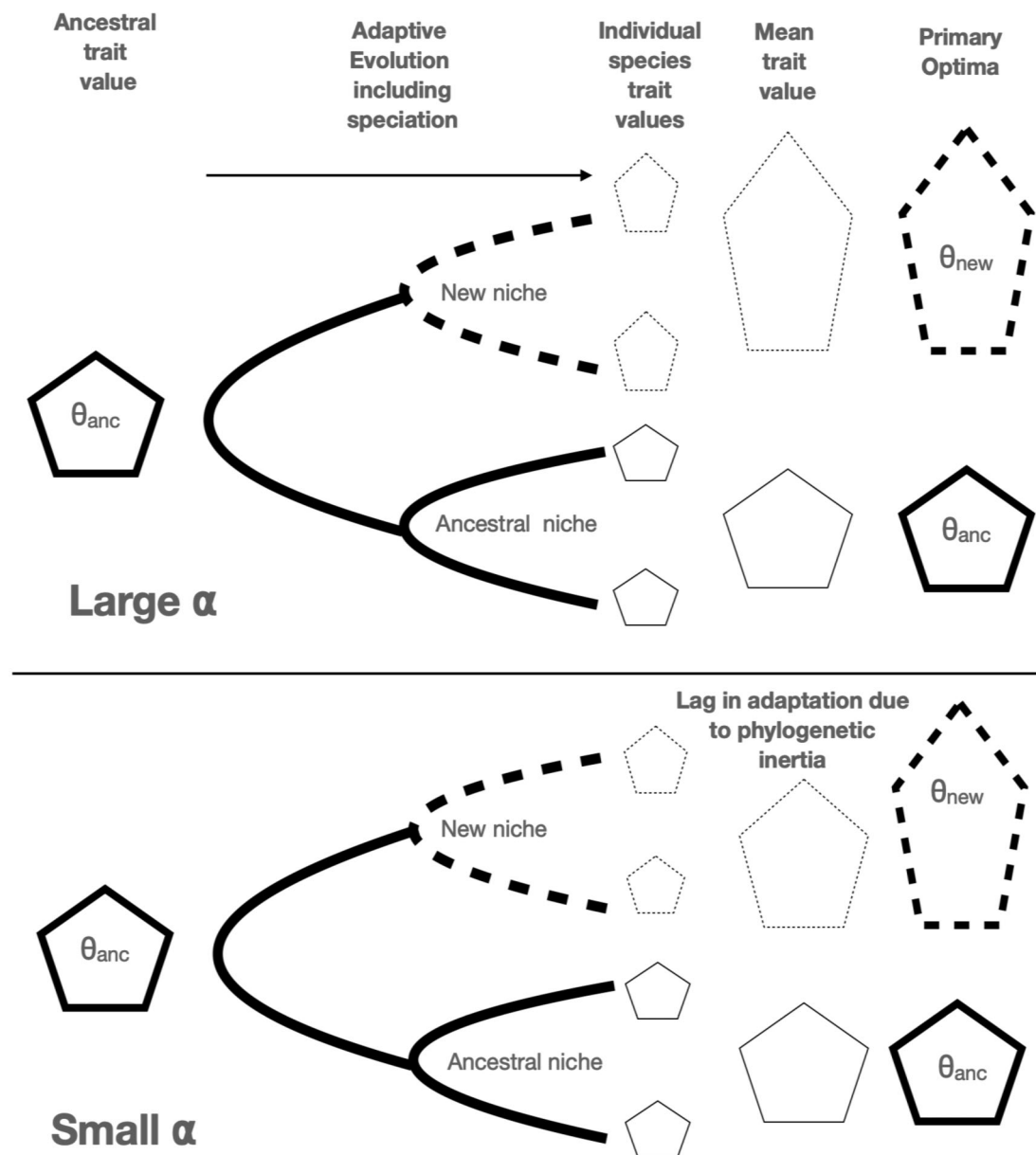


Figure 1. Inertia affects trait evolution on a phylogeny. The trait is represented by a pentagon, and differential selection as two niches (dashed and solid lines). The niche represented by the solid line is also the ancestral niche (anc), thus stabilizing selection acts continuously on the species that remain in this niche. The dashed line represents a niche that has an elongated pentagon as a primary optimum (θ_{new}). With low phylogenetic inertia (top panel, large α) the new phenotypic space represented by the primary optimum associated with the dashed line niche is quickly reached on average. With strong inertia (bottom panel, small α), trait evolution is constrained by contingency, and it takes much longer to reach the phenotypic space around the primary optimum for the new niche.

each species i , given by

$$\hat{y}_i = c_{0i}y_a + c_{1i}\theta(x_1) + c_{2i}\theta(x_2) + \dots + c_{ki}\theta(x_k), \quad (2)$$

where y_a is the ancestral state at the root of the phylogeny, $\theta(x_1)$ is the primary optimum for state x_1 of the environmental variable, $\theta(x_2)$ is the primary optimum for state x_2 of the environmental variable, and so on for all k possible states of the environment. The coefficients c_{ji} represent the influence of environmental state j on species i and are functions of α and the history of association between j and i , as described in Hansen (1997). They are all between zero and one, and they sum to one. The coefficient corresponding to a particular environmental state will be large when the species has spent a lot of its history associated with this state, with re-

cent associations weighted more heavily. The larger the rate of adaptation, α , the more the weighting shifts towards recent environments, and when α approaches infinity, adaptation is instantaneous and only the current environment is weighted (Figure 1).

If the environmental states, the x_j 's, are mapped on the phylogeny, the c_{ji} 's may be computed, and the $\theta(x_j)$'s can be estimated in a linear model framework analogous to an ANOVA or regression model. For non-ultrametric trees, such as those that include extinct species fossil data, the ancestral trait state, y_a can also be estimated as detailed in Hansen (1997) and Hansen et al. (2008). Due to phylogenetic structure, we must account for non-independence in residual deviations from the predicted values using estimation techniques such as general-

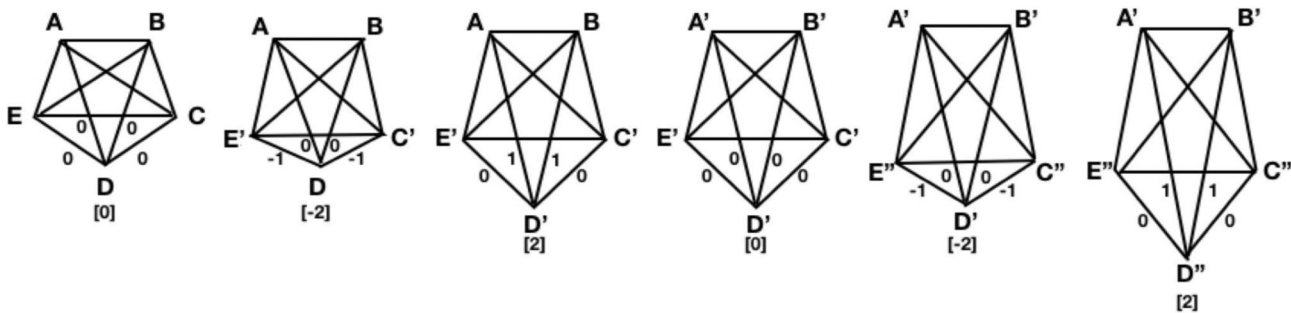


Figure 2. Correlated-progression model adapted from [Kemp \(2007\)](#). Elongation of a shape through a succession of evolutionary steps involving five phenotypic traits (A–D). As in [Kemp \(2007\)](#), the traits are assumed to be mutually interconnected by slightly flexible functional linkages represented by the lines. Changes in trait pairs A and B, as well as E and C are highly correlated to preserve bilateral symmetry. All traits can evolve (i.e., change X-Y coordinates in the figure), but only by one increment at a time. Traits can also only be one increment ahead of any connected traits at any one time. Evolvability of a given trait is indicated by the sum of its linkage values (shown above in square brackets for trait D), where lower values indicate less constraint and therefore a higher probability of further change.

ized least squares or maximum likelihood. The residual covariances (given in the [online Appendix](#)) are dependent on the rate of adaptation, α , and are larger when the rate of adaptation is small. Note that both the design matrix and residual covariance depend on α and cannot be parameterized independently of one another. In summary, the method fits a linear model conditional on α to a vector of species means \mathbf{y} , given as

$$\mathbf{y} = \mathbf{C}\theta + \mathbf{r}, \quad \mathbf{r} \sim N(0, \mathbf{V}) \quad (3)$$

where \mathbf{C} is a design matrix with elements c_{ij} , θ is a vector of primary optima to be estimated, one for each niche (plus the ancestral state in some cases), \mathbf{r} is a vector of residuals for each species, which follows a multivariate normal distribution with a variance matrix, \mathbf{V} , with elements given in the [online Appendix](#). The elements of both \mathbf{C} and \mathbf{V} depend on the phylogeny and the parameter α , and those of \mathbf{V} also depend on σ .

Interpreting the parameters

The adaptation-inertia model is sometimes presented as being based on [Lande's \(1976\)](#) selection-drift model ([Butler & King, 2004](#); [Lajeunesse, 2011](#); [Martins, 2000](#)). As mentioned in the introduction, this interpretation was explicitly rejected by [Hansen \(1997\)](#) with the argument that it makes little sense on the time scales of typical among-species comparative data. It is now well established that strengths of selection, evolvability, and rates of microevolution are so high that evolution on a constant adaptive landscape would appear instantaneous on time scales beyond a few hundred generations (e.g., [Hansen & Pélabon, 2021](#)). The widespread observation of phylogenetic signal on million-year time scales thus implies a certain decoupling of micro- and macroevolution and requires specific interpretation in macroevolutionary terms (see [Hansen, 2024](#) for more detail). The simple drift-selection interpretation may, however, be relevant in cases in which time scales are much shorter, as in some fossil time series, or possibly for categories of traits, such as gene expression or aspects of genome architecture, that may be under extremely weak selection. If the focus is on explaining species differences in morphology, physiology, or life-history traits, however, a dynamic adaptive landscape must be considered.

The adaptation-inertia model incorporates this with the premise that adaptive peaks themselves change over time and

that it is a lag in adaptation to the changing peaks that generates the phylogenetic inertia component of observed phylogenetic correlations in traits. Although this interpretation is undeniably vaguer and less well connected to population genetic first principles than quantitative genetic models, it is crucial for understanding how microevolutionary processes might generate macroevolutionary patterns ([Hansen, 2012, 2024](#)). The key parameters, α , σ , and θ_i in the model consequently cannot be interpreted in population genetic terms but need specific macroevolutionary interpretations, as when θ is interpreted as a primary optimum. The other parameters have the following macroevolutionary interpretations:

The Alpha (α) Parameter: Rate of Adaptation and Phylogenetic Half-Life—[Hansen \(1997\)](#) described α as a rate of adaptation, indicating how quickly a trait approaches its primary optimum. [Simpson \(1944\)](#) and [Kemp \(1982, 2006, 2007\)](#) suggested that adaptation towards optima might be slow due to what Kemp termed the correlated-progression hypothesis. This idea posits that a focal trait is embedded in a network of coadapted traits. Large changes might initially be detrimental due to internal selective constraints. Instead, small changes in the focal trait cause adjustments in other traits, which then permit further small changes in the focal trait, creating a slow, correlated progression. Thus, a small α could signify strong internal selective constraints (Figure 2).

To aid interpretation, [Hansen \(1997\)](#) suggested that α can be expressed as a phylogenetic half-life ($t_{1/2} = \ln(2)/\alpha$), which has the same units as the branch lengths of the phylogenetic tree. This represents the time it takes for a trait to move half the distance from its ancestral state to a new primary optimum. This half-life is invariant to the original distance to the primary optimum because the model is set up to let the rate of approach to the primary optimum increase linearly with distance from it. A large half-life relative to tree height, implies substantial phylogenetic inertia, meaning that species trait values are likely to lag their optimal states, and strong phylogenetic correlations exist between species. If a single primary optimum is modelled across the entire phylogeny, this half-life also serves as a general measure of phylogenetic signal.

The Sigma (σ) Parameter: Stochastic Movement and Stationary Variance—The σ parameter, with units of trait units per square root of time units, quantifies the amount of stochastic (random) movement in adaptive peaks that is not deterministically related to the primary optimum. A large σ might indicate more change in other unmeasured selective factors in

fluencing local adaptive peak positions. When the Ornstein–Uhlenbeck process reaches a stochastic equilibrium, the stationary variance among species ($\nu = \sigma^2/2\alpha$) represents the balance between the primary selective force (the pull to the primary optimum) and all other secondary, unmeasured selective, and random forces (of which genetic drift is only one of several). A large ν suggests a substantial amount of residual variance not explained by the primary optima. Ultimately, it may be easier to interpret the phylogenetic half-life ($t_{1/2}$) and stationary variance (ν) directly, as they contain the same information as α and σ but offer a more intuitive relation to the macroevolutionary process.

The arguments above pertain to traits that are tightly linked to fitness, but what about traits that are under weak selection over long periods of time, such as gene expression levels or protein stability? Eukaryotic protein fitness landscapes, for example, can sometimes stay stable for extended periods (e.g., Latrille et al., 2024) when conserved, non-intrinsically disordered proteins have a single long-term primary fitness optimum related to maximum stability. In such cases, any observed “lag” in adaptation (or conversely phylogenetic inertia) probably does result from very weak selection on a stable landscape with a single global optimum, not a dynamic one. Therefore, interpreting such a lag within an “adaptation-inertia” framework, which assumes a constantly changing landscape, can be misleading in these cases, and we caution that interpretation of the model parameters should be based on the likely trait dynamics and the time scale in question.

Modelling the primary optimum: approaches and challenges

The adaptation-inertia framework models how species’ traits evolve towards primary optima within adaptive zones. Initially, this involved using phylogenetic character reconstruction or paleobiological information to map environmental variables onto the phylogeny.

Fixed, categorical niches and model selection

Butler & King (2004) advanced this by treating environmental variable assignments on the phylogeny as hypotheses, developing the OUCH (Ornstein–Uhlenbeck models for Comparative Hypotheses) R package (see also Hipp & Escudero (2010) for extensions that take variable assignment error into account). They used information-based model-selection criteria (Burnham & Anderson, 1998), like Akaike information criterion (AIC), to evaluate different arrangements of fixed, categorical environmental variables and count as parameters all the primary optima, α and σ (initially a separate ancestral trait value at the root of the tree was also estimated, but this subsequently got wrapped into one of the existing primary optima to avoid estimation issues on ultrametric trees). AIC has several advantages over traditional significance testing because it avoids arbitrary null hypotheses, allows comparison of non-nested models, and can compare models with the same niches with different mappings on the phylogeny (Lajeunesse, 2009; Posada & Buckley, 2004). For smaller datasets, AICc (a small-sample correction) (Hurvich & Tsai, 1989) is recommended. Models are ranked by their AIC values, with $\Delta\text{AIC} > 2$ (i.e., when the difference between a given model and the best model’s AIC is greater than 2) indicating substantially weaker support compared to the best model (Burnham & Anderson,

2004). Since then, increasingly sophisticated methods to detect shifts in primary optima along phylogenies have been developed:

- Ingram & Mahler (2013) introduced a stepwise AIC approach in their SURFACE (Surface Uses Regime Fitting with AIC to model Convergent Evolution) R package to find and collapse convergent niches into single niches.
- Ho & Ané (2014), however, noted that stepwise AIC can over-parameterize models and proposed using a wider range of information criteria that more heavily penalize complexity in their PHYLOLM (PHYLOgenetic Linear Modelling) R package.
- Uyeda et al. (2014) and Catalán et al. (2019) adopted a Bayesian approach [implemented in the BAYOU (Bayesian Ornstein–Uhlenbeck models) R package and in RevBayes] to tackle over-parameterization by incorporating prior information (e.g., fossil data) and using reversible jump MCMC for regime shift detection.
- Khabbazian et al. (2016) applied Tibshirani’s (1996) lasso method (in the l1OU R package) for faster detection of optima shifts, enabling analysis on very large phylogenies.

Despite these statistical advancements including those that allow for rate shifts in different parts of the tree e.g., Beaulieu et al. (2012), PHYLOGENETICEM (Bastide et al., 2017; Bastide et al., 2018) and PCMBASE (Mitov et al., 2020), it is crucial to remember that even statistically well-supported hypotheses for predictor arrangements on a phylogeny should be critically evaluated for biological plausibility of the estimated primary optima. Uyeda et al. (2018) provide a thoughtful perspective on what they term hypothesis testing (motivated by biologically plausible alternatives and a search for causation) and data-driven (motivated by automatic niche-shift detection and description of macroevolutionary patterns) approaches and how both are susceptible to bias from singular evolutionary events. Motivated by Beaulieu and O’Meara’s (2016) application of hidden-state model principles to models of trait evolution, where background shifts in evolutionary regimes unrelated to the focal traits are accounted for, Uyeda et al. (2018) argue that the two approaches can be combined into a more powerful approach for hypothesis testing, an argument that we agree with wholeheartedly. Based on May & Moore’s (2020) mathematical groundwork, Boyko et al. (2023) have recently extended the methods to allow for the modelling of correlations between continuous and discrete traits with a joint Ornstein–Uhlenbeck Hidden-Markov process. These developments are implemented in Beaulieu & O’Meara’s (2025) OUwie R package. Additionally, fitting layered Ornstein–Uhlenbeck models to evolutionary time series can provide further insights into adaptive landscape dynamics and how well lineages track changes in adaptive peaks over macroevolutionary timescales (Hunt et al., 2008; Reitan et al., 2012; Voje, 2020, 2023; Holstad et al., 2024).

Moen et al. (2016) developed a method to better understand why species’ traits deviate from their primary optima. They separate the variation around current primary optima into two parts: random deviations around current primary optima and systematic deviations caused by adaptation to past environments. This allows for quantifying how much past environments hinder adaptation to present ones. They did this by breaking down the total variation of trait values (TSS) around their estimated primary optima into three components

as follows:

$$\begin{aligned}
 \text{TSS} &= \sum_{i=1}^k \sum_{j=1}^{n_i} (y_{ij} - \theta_i)^2, \\
 &= \sum_{i=1}^k \sum_{j=1}^{n_i} ((y_{ij} - \bar{y}_i) + (\bar{y}_i - \theta_i))^2, \\
 &= \sum_{i=1}^k \sum_{j=1}^{n_i} (y_{ij} - \bar{y}_i)^2 + \sum_{i=1}^k n_i (\bar{y}_i - \theta_i)^2 \\
 &\quad + 2 \sum_{i=1}^k \sum_{j=1}^{n_i} (y_{ij} - \bar{y}_i) (\bar{y}_i - \theta_i). \tag{4}
 \end{aligned}$$

The first term of the decomposition, or Sum of Squared Deviations due to Random, Current Environmental Influences (SSE) measures the variation in trait values among species living in the same current environment. The second term, or Sum of Squared Deviations due to History (SSH), measures the difference between average trait values and the primary optimal traits, reflecting historical influences. The third term is the covariance between the first two terms that can be ignored in the subsequent arguments as it cancels to zero upon rearrangement of its sums. Mean squares are obtained for SSE (current environmental influences) and SSH (historical deviations) by dividing each by their degrees of freedom [(respectively, the number of species—the number of environments, and the number of environments—(1)], which can then be squared to obtain variances. By comparing the variances derived from SSH and SSE, researchers can determine the primary driver of trait inertia. If the SSH-based variance is larger, it means adaptation to different past environments has a greater influence on traits within a niche than their current environment. Conversely, if SSE-based variance is larger, clade membership (shared ancestry) has a stronger influence on inertia.

For instance, Moen et al. (2016) studied 167 frog species across ten microhabitats. After removing size effects (the first principal component after dimension reduction of various traits), they found that for traits related to locomotion, the variance due to history (SSH) was significantly larger than that from random current effects (SSE). This suggests that incomplete adaptation as frogs transitioned between niches, rather than current environmental factors, largely explains why similar phenotypes do not perfectly converge in similar niches across different geographic locations.

Runaway primary optima, infinite phylogenetic half-lives, and the Brownian motion with a trend

When a phylogenetic half-life approaches infinity at the same time as estimated primary optima become infinitely distant from current species values, it does not necessarily mean traits are not adapting. Instead, Hansen (1997) argued that this situation requires a reparameterization of the Ornstein–Uhlenbeck process. In such cases, the model transforms into a Brownian motion with niche-specific, deterministic trends, which can be reliably estimated as $\tau_i = \lim_{\alpha \rightarrow 0} \alpha \theta_i$, the average trait change per time as α approaches 0. The compositive parameters τ_i , which also depend on the amount of time the traits have been evolving in separate niches, can be reliably estimated on non-ultrametric trees, even when α or the θ_i are individually inaccurate. These niche-specific trends are biologically interpreted as niche-specific rates of adaptation to distant, unobtainable optima, where the σ^2 parameter measures

the magnitude of the perturbing forces. On ultrametric trees, the τ_i can only be estimated as contrasts such as τ_i , τ_j between niches i and j (see Grabowski et al., 2023 for a recent example).

Although less common than other trait dynamics, trends in fossil time series do occur (Hunt, 2007; Hunt et al., 2015; Voje, 2016). Hunt (2006) demonstrated that when such evolutionary transitions follow a Gaussian distribution, a Brownian motion with a trend can be used to model the dynamics. In these cases, the mean (μ) dictates the direction and strength of trait evolution, and the variance (σ^2) captures stochastic fluctuations around this trend. This model predicts that the expected change between ancestor and descendant populations after time t is normally distributed with a mean of $t\mu$ and a variance of $t\sigma^2$.

Modelling primary optima on continuous, randomly evolving niche variables

The adaptation-inertia framework has been extended beyond fixed, categorical niches (like in an ANOVA, Figure 3A) to model primary optima as continuous variables. To begin with, we can let the primary optimum depend on a continuous environmental variable (x). Assuming a linear relationship, this becomes a linear regression:

$$\theta(x) = a + bx. \tag{5}$$

Here, a is the intercept and b is the slope. A non-zero slope suggests the primary optimum is influenced by x , which could be consistent with adaptation. If the predictor variable's historical states can be reliably mapped onto the phylogeny, this can be fitted in much the same way as the ANOVA-like model described above (Hansen, 1997). However, mapping continuous predictors with fixed historical states is often problematic. Hansen et al. (2008) proposed treating the predictor variable itself as a randomly evolving variable, requiring only its end states (Figure 3B). They suggested a Brownian motion model for the predictor:

$$\begin{aligned}
 dy &= -\alpha(y - (a + bx))dt + \sigma_y dW_y, \\
 dx &= \sigma_x dW_x. \tag{6}
 \end{aligned}$$

In this setup, the first equation describes an Ornstein–Uhlenbeck process for trait y around a primary optimum that is a linear function of predictor x . The second equation states that x marginally follows a standard Brownian motion, where dW_x and dW_y are independent white-noise processes, and σ_x quantifies the stochastic change in x .

The conditional expectation for this model is

$$\hat{y}_i = k + \rho b x_i, \tag{7}$$

where k is an intercept term influenced by several parameters (see [online Appendix](#)) and

$$\rho = 1 - (1 - e^{-\alpha t_i}) / \alpha t_i \tag{8}$$

is a phylogenetic correction factor that accounts for phylogenetic inertia. Here, t_i is the time from the root to species i . The model estimates an “optimal” regression slope (b) and an “evolutionary” regression slope (ρb). Since ρ is between 0 and 1, it predicts that the observed evolutionary regression will be shallower than the optimal regression due to phylogenetic inertia. A shallow observed slope could thus mean either a genuinely shallow optimal relationship or that species are simply lagging in their adaptation to a steeper one. The time dependence of ρ predicts that evolutionary regression slopes will typically be shallower at lower taxonomic levels (Burt,

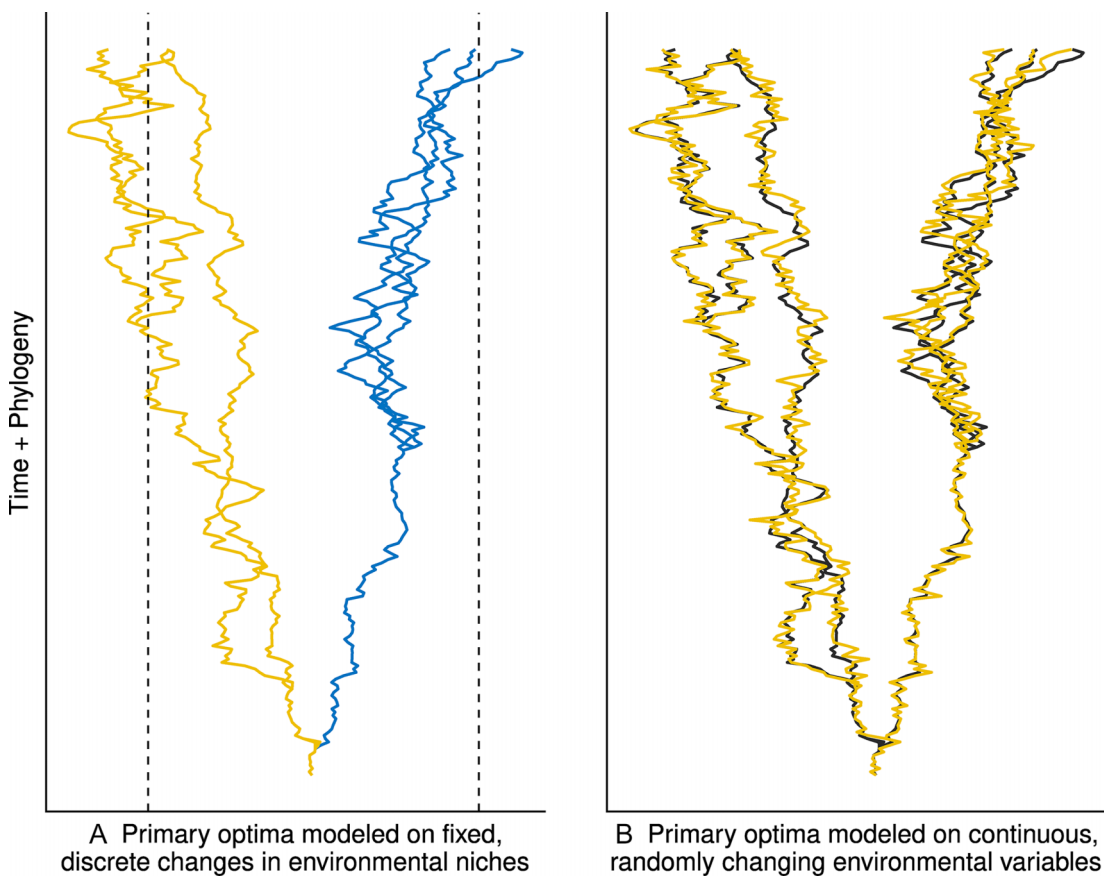


Figure 3. Trait evolution for six species on a phylogeny where (A) the trait is modelled as an Ornstein–Uhlenbeck process with two primary optima that are dependent on fixed, categorical states of an environmental variable (represented by the two dashed lines on the X axis, which represents an arbitrary range of ordered trait values) and (B) the optima depend on a continuous variable that itself randomly evolves on the phylogeny (solid black line). Note that in B, both the optima (black line) and trait have a stochastic variance component to their evolution (as indicated by random shifts on the X, trait-value axis), but also that the trait tracks the optima closely as the process was simulated with a small half-life and a regression slope representing a $\sim 1:1$ between trait and the environmental variable.

1989; Deaner & Nunn, 1999; Hansen & Bartoszek, 2012), a commonly observed pattern (Martin & Harvey, 1985).

The residual covariances in this “random-effect” model are more complex than in the fixed-effects model and are provided in the [online Appendix](#). These models have also been generalized to include multiple predictors (Hansen et al., 2008; Labra et al., 2009) and trends in the underlying Brownian motion for the primary optima, as implemented in the latest SLOUCH (Stochastic Linear Ornstein–Uhlenbeck models for Comparative Hypotheses) R package (Kopperud et al., 2020). Fixed and random effects can be combined by replacing the intercept k with the fixed primary optima from Equation 2, while maintaining the random-effect residual covariance. A continuous covariate without any phylogenetic covariance structure can also be fit as a direct effects regression (Grabowski et al., 2016)—this is useful when direct scaling effects, such as increases in a trait value simply because it scales mechanically with body size, need to be incorporated.

We note that although Ives and Garland (2010, 2014) have previously introduced a logistic regression based on the Ornstein–Uhlenbeck process, they separated the modelling of stochastic residuals from the mean structure of the model, which as discussed above, does not capture what the adaptation-inertia methods set out to do; thus a logistic regression in the adaptation-inertia framework remains to be developed. A summary of the various estimated parameters for the

univariate models is provided in [Table 1](#). The various software packages for implementing the methods in the “adaptation inertia” framework are reviewed elsewhere (Fuentes-González, in review).

Multivariate extensions

Understanding trait evolution often requires analyzing interactions between traits, crucial for phenomena like phenotypic integration and evolutionary trade-offs Armbruster et al., (2014). While univariate analyses can offer limited insight into trait interaction dynamics by swapping predictor/response roles, they typically miss the full picture of trait interactions. Reducing multivariate traits to single dimensions before phylogenetic analysis can also obscure vital evolutionary components (Uyeda et al., 2015).

Developing fully multivariate models is complex due to issues with likelihood functions and reliance on matrix calculus, making implementation and parameter interpretation challenging. Early multivariate adaptation-inertia models simplified assumptions (King & Butler, 2009) that were subsequently relaxed (Bartoszek, 2012; Clavel, 2015; Mitov et al., 2019) into a more general multivariate comparative method based on the Ornstein–Uhlenbeck process, described by the following stochastic differential equation:

$$dy(t) = -A(y(t) - \theta(t))dt + \Sigma dW(t). \quad (9)$$

Table 1. A summary of the commonly interpreted parameters estimated for the univariate Ornstein–Uhlenbeck models.

Parameter	Definition
α	Controls how fast a trait reaches a primary optimum in expectation
b	The optimal regression slope for the relationship between a trait and a continuous, randomly evolving environmental variable
ρ	A Phylogenetic correction factor. The evolutionary (generalized least squares) regression slope for the relationship between a trait and a continuous, randomly evolving environmental variable is a composite parameter consisting of the optimal regression slope (b) multiplied by the phylogenetic correction factor (ρ , see main text for details)
σ^2_y	The instantaneous variance (rate of change due to stochastic influences) of the trait being modelled by an Ornstein–Uhlenbeck process
θ_i	Primary optima, modelled on fixed, categorical predictors describing a niche for which the ancestral states are typically reconstructed on the phylogeny. This is the mean expected adaptive trait value for groups of species evolving in the same niche or adaptive zone
$t_{1/2} = (\ln 2/\alpha)$	Phylogenetic half-life—a non-linear transformation of α that allows one to interpret the degree of phylogenetic inertia on the same scale as the phylogenetic branch lengths. Interpreted as the “time” it takes for half the influence of ancestral state values to disappear from current trait values as they evolve towards their niche optima. Also used as an estimate of phylogenetic signal when a single niche optimum is modelled for the entire tree
$\nu_y (= \sigma^2_y/2\alpha)$	Stationary variance of a trait’s evolution (i.e., the variance once the process has stabilized after a long time) should the predictors of the model be fixed and not randomly evolving

Here, the scalar trait values (y) and primary optimum (θ) from the univariate model in Equation 1 become vectors, and \mathbf{W} is a multi-dimensional Brownian motion. The univariate stochastic movement (σ) and rate of adaptation (α) parameters are replaced by a Σ matrix and an \mathbf{A} matrix, respectively. The Σ matrix mediates potentially correlated stochastic perturbations to each trait.

The generalized, fully parameterizable \mathbf{A} matrix offers significant advantages for interpreting multivariate trait adaptation, allowing tests of various hypotheses about evolutionary interactions. The real part of \mathbf{A} ’s eigenvalues acts like the univariate α parameter, determining the joint rate of trait convergence to their stationary distribution. When transformed as $\ln(2)/\text{eigenvalue}$, each transformed eigenvalue represents the phylogenetic half-life for a particular dimension of multivariate trait evolution. Off-diagonal entries of \mathbf{A} show how one trait’s approach to its optimum affects other traits’ evolutionary trajectories. A diagonal \mathbf{A} matrix implies traits adapt independently to environmentally determined primary optima. A nondiagonal \mathbf{A} matrix means traits influence each other’s primary optima. Upper or lower triangular \mathbf{A} matrices model unidirectional influences. Below, we describe, by means of example, how the \mathbf{A} matrix of the currently available methods can potentially be used to infer coevolutionary processes.

For non-deterministic influences, a diagonal Σ matrix indicates independent stochastic effects on each trait’s evolution. Triangular Σ matrices model interactions between these stochastic influences, which can arise from shared developmental constraints, pleiotropy, or linkage disequilibrium with unmeasured traits under selection. These concepts are detailed in a series of recent studies (Bartoszek et al., 2023a, 2023b; Bartoszek et al., 2024).

A biological example: figs and their pollinating wasps

The biological example

Weiblen (2004) studied the correlated evolution of ovipositor lengths in fig wasps and style lengths of fig flowers that the wasps lay their eggs in. These respective lengths must closely match to allow for successful egg laying as the wasps must in-

sert their ovipositors into the styles and be able to reach and lay their eggs specifically between the integument and nucellus for them to successfully hatch. Using phylogenetic independent contrasts, Weiblen (2004) showed that changes in these traits are more strongly correlated with each other than with phylogenetic position or body size. This example provides us with an opportunity to showcase the additional information that can be gained through the adaptation-inertia framework with its focus on parameter interpretation and ability to model dynamic adaptive landscapes in different ways. For the sake of brevity, we provide only the key parameter estimates and a verbal description of their interpretation. The full repertoire of parameters estimated, confidence in the estimates, and an interpretive description, along with the R code used to implement all models, is given in the [Supplementary Material](#).

Fixed, categorical regimes analysis

As Weiblen (2004), we investigated if fig wasp ovipositor length adapts to the style length of their host figs, expecting shorter ovipositors in wasps pollinating dioecious figs (which generally have shorter styles) compared to those pollinating monoecious figs (with longer styles). Using maximum likelihood to reconstruct fig host states on the pollinator phylogeny (Figure 4), we fitted an Ornstein–Uhlenbeck model with two primary optima for ovipositor length (corresponding to monoecious and dioecious hosts). This two-optima model outperformed both Brownian motion and a single-optimum model ($\Delta\text{AIC}_c = 36.44$ and 24.65 , respectively), explaining 62% of the variance. The two-optima model showed a phylogenetic half-life of essentially zero (best estimate = 0.0 with 0.0 to 3.8% of tree height 2-log-likelihood support interval). Based on the time-scaled cladogram presented in Cruaud et al. (2012), the genera studied here had a common ancestor 75.1 mya, indicating that in years, the phylogenetic half-life estimate falls between 0.0 and 2.6 million years with a best estimate of 0.0 years, indicating that species’ traits closely track shifts in primary optima with little lag. In contrast, a single-optimum model estimated a phylogenetic half-life of 8.5% of tree height, or 6.3 million years, where the support interval excludes 0 (3.0 to 18.8 my). This demonstrates that the phylogenetic signal observed in simpler models largely reflects

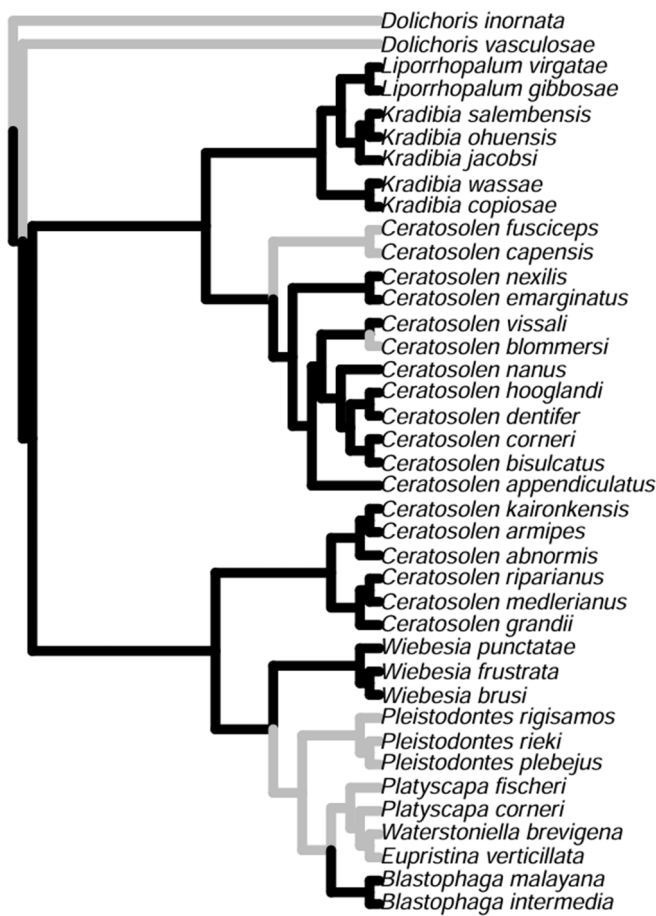


Figure 4. Phylogeny (from Weiblen, 2004, estimated from 18s rRNA sequences, made ultrametric and scaled to a height of 1) representing the relationships between the fig wasps studied here and an ancestral state reconstruction (see main text for details) of whether they pollinate dioecious (black) or monoecious (gray) fig trees.

adaptive evolution to phylogenetically structured optima, cautioning against removing all phylogenetic signal in analyses as it can inadvertently erase adaptive effects

The estimated primary optima for ovipositor length were 0.31 ± 0.04 mm for dioecious fig pollinators and 0.88 ± 0.06 mm for monoecious fig pollinators. Although the measured average fig style lengths (0.54 mm for dioecious, 1.25 mm for monoecious) were slightly longer than ovipositors (likely due to measuring mature figs rather than those receptive to pollination), the substantial difference between the two ovipositor optima strongly supports our hypothesis. The estimated stationary variance was 0.04 mm^2 , meaning species were, on average, within $\sqrt{2v/\pi} = 0.16$ mm of their primary optima. This difference suggests that the average dioecious fig pollinator would struggle to lay eggs in monoecious figs and vice versa, highlighting the precise adaptation.

Convergent evolution inertia decomposition

Although our best estimate for the phylogenetic half-life was zero (implying traits perfectly track their optima), we can still demonstrate Moen et al.'s decomposition of deviations to illustrate its utility. When forcing the phylogenetic half-life to be 10% of tree height, we calculated the mean ovipositor lengths for wasps pollinating dioecious figs as 0.31 mm (optimum:

0.30 mm) and for monoecious figs as 0.87 mm (optimum: 0.96 mm). Our analyses show the ancestral state was dioecious fig pollination, with five transitions to monoecious pollination among the 39 lineages. Using these values, the sum of squared deviations due to random, current environmental influences (SSE) was 5.14 mm^2 , and the sum of squared deviations due to history (SSH) was 0.08 mm^2 . After dividing by their degrees of freedom, their mean squares were 5.14 mm^2 and 0.002 mm^2 , respectively. Comparing these variances, we would conclude that clade membership influences the distance from primary optima far more than adaptation to historical habitats. This result makes intuitive sense given our finding of a zero phylogenetic half-life in the actual best-fit model, because when there is no lag, historical adaptation does not hinder current adaptation.

Randomly evolving environment analysis

To explicitly test if ovipositor length adapts directly to style length, we used style length as a continuous, randomly evolving predictor for ovipositor length optima, modelling it as a Brownian motion with ovipositor length tracking it via an Ornstein–Uhlenbeck process (Hansen et al., 2008). This model yielded a significantly better fit than the previous best 2-fixed optima model ($\Delta\text{AIC}_c = 27.54$), explaining 80% of the variance. The estimated phylogenetic half-life was remarkably short: 0.07% of tree height [$\sim 50,000$ years, support interval = 0.0–3.8 my (Figure 5)], indicating rapid adaptation. This contrasts sharply with the 9.3-million-year half-life of a global-optimum model, reinforcing that most phylogenetic signal stems from phylogenetically structured niches rather than inherent inertia. The estimated optimal relationship between ovipositor and style length (Figure 5) showed a regression slope of 0.75 ± 0.06 , nearly identical to the evolutionary regression slope (0.74 ± 0.06) and the ordinary least squares slope (0.74 ± 0.06). This congruence is expected given the short phylogenetic half-life, meaning current trait values are very close to their optima. The estimated stationary variance was 0.02 mm^2 , corresponding to an average deviation of approximately 0.11 mm from the optima. With the 95% confidence interval for the optimal slope (0.62 to 0.86 mm) excluding zero, and style length explaining 80% of ovipositor length variance, we conclude that style length has a large and statistically significant effect on ovipositor length optima. Furthermore, the short phylogenetic half-life (50,000 years) relative to the tree height indicates that ovipositor length adapts rapidly to changes in fig style length.

Mixed-model and multiple regression analysis

To determine if ovipositor length adapts primarily to style length or also to fig reproductive mode, we fitted an ANCOVA-style mixed model. This model, which combines a fixed categorical predictor (reproductive mode) with a randomly evolving continuous predictor (style length), was nearly as well-supported as our best model ($\Delta\text{AIC}_c = 0.64$). Examining the estimated intercepts for this mixed model, however (Dioecious: -0.03 ± 0.06 mm; Monoecious: 0.09 ± 0.12 mm), their overlapping 95% confidence intervals suggest that fig reproductive mode itself does not significantly influence primary optima beyond the effect of style length.

Following Weiblen's (2004) approach, we then used multiple regression in SLOUCH to assess if wasp body size (thorax width) also predicts ovipositor length. We treated body size

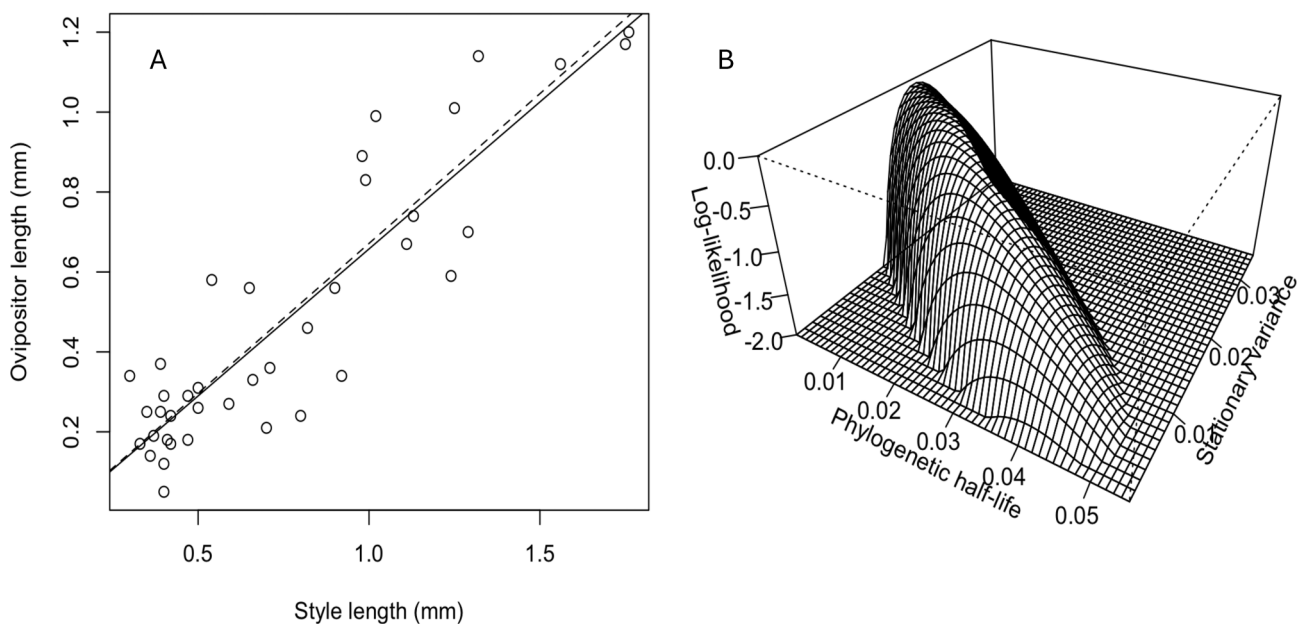


Figure 5. (A) Optimal (dashed line) and evolutionary (solid line) regressions for fig wasp ovipositor length modelled on randomly evolving fig style length. (B) The 2-unit log-likelihood support surface for the phylogenetic half-life and stationary variance for the regression model applied in A.

as a fixed covariate, as we wanted to test direct, mechanical scaling effects. The multiple regression model, including fixed body size and randomly evolving style length, yielded a non-significant direct thorax-width slope (-0.003 ± 0.12). It was also $\Delta AIC_c = 2.62$ units worse than the best single-predictor (randomly evolving style length) model, and it only explained an additional 1% of variance (total 81%). A model with only fixed body size as a predictor was far worse ($\Delta AIC_c = 52.43$) than the best model, explaining only about 6% of the variance. Thus, consistent with Weiblen (2004), our univariate analyses confirm that style length is the single most important influence on the adaptive optima for ovipositor lengths among all predictors considered.

Multivariate analysis

Weiblen (2004) emphasized the coevolutionary nature of ovipositor and style length evolution, and thus far, we have been modelling the relationship between them as one in which the latter evolves independently of the former. An implied assumption of this approach is that ovipositor length tracks the evolution of style length, but not vice versa. The alternative can be studied by fitting the same model but with switched variables, i.e., ovipositor length evolving randomly in the phylogeny as a Brownian motion with style length tracking it through an Ornstein–Uhlenbeck process. Although this switched variable approach can offer insights into the directionality of the pattern (Davis et al., 2012; Pienaar et al., 2013), it is still restrictive in the sense that one of the variables is forced to evolve independently of the other. Considering that figs depend solely on fig wasps for their pollination, this restriction is undesirable as it excludes the possibility that ovipositor and style length are reciprocally exerting selection on each other [i.e., it leaves out reciprocal selection, which is at the core of textbook definitions of coevolution e.g., Futuyma & Kirkpatrick (2023)]. A multivariate approach is better suited to address this type of specific coevolution hypothesis because it makes less assumptions about how the vari-

ables evolve, allowing for the possibility that both traits influence each other's evolutionary trajectory. This possibility is facilitated by modelling each variable as an Ornstein–Uhlenbeck process where the primary optima are allowed to reciprocally influence each other. The mvSLOUCH R package (Bartoszek et al., 2012) allows for contrasting four general scenarios for this analysis with information criteria: (i) as in Hansen et al. (2008) one trait is modelled as an Ornstein–Uhlenbeck process tracking an optimum affected by one or more other traits each modelled as a Brownian motion process, henceforth the “OUBM” model; (ii) vice versa (i.e., the OUBM model with switched variables); (iii) a model in which the trait values, as well as the association between the two traits is mediated by stochastic perturbations only (i.e., as a multivariate Brownian motion process, henceforth “BMBM” model); (iv) a model in which both traits are modelled as an Ornstein–Uhlenbeck process (i.e., as a multivariate Ornstein–Uhlenbeck process as described above, henceforth the “OUOU” model) each with their own primary optimum. To test for coevolution specifically, we can parametrize the OUOU models in such a way that the two traits' primary optima reciprocally affect each other's dynamics. When more variables and more hypotheses are available, any custom model can be built from any combination of these four general scenarios, and fixed categorical predictors can also be included, but for the fig wasp example, we are only interested in (1) whether the specific coevolution model (an OUOU model with symmetric off-diagonal elements in the A matrix as discussed below) outperforms the others and (2) if so, how do we interpret the parameter estimates?

The more nuanced multivariate approach requires contrasting various matrix parameterizations to determine whether the associations between traits are mediated through the stochastic perturbations (through non-zero off-diagonals in Σ), coadaptation (through non-zero off-diagonals in A), or both. For the fig-wasp example, the best fitting candidate (by AIC_c criteria, Table 2 and Supplementary Material) was an OUOU model parameterization with non-zero, equal-value-

Table 2. Hypothesis testing for multivariate scenarios.

Hypothesis	Model	A-matrix	Σ -matrix	AICc	r
Specific coevolution	OUOU	Symmetric-positive-definite	Single-value-diagonal	0.85	0.90
Style primary optimum affects ovipositor primary optimum	OUOU	Upper-triangular	Single-value-diagonal	2.44	0.90
Ovipositor primary optimum affects style primary optimum	OUOU	Lower triangular	Single-value-diagonal	2.64	0.90
Adaptation to independent primary optima with stochastically generated correlation	OUOU	Single-value-diagonal	Upper-triangular	8.95	0.90
Style adapts to randomly evolving ovipositor	OUBM	Scalar	Scalar	10.89	0.97
Ovipositor adapts to randomly evolving style	OUBM	Scalar	Scalar	10.91	0.97
Correlated evolution without adaptation to primary optima	BMBM	-	Lower triangular	44.39	0.76

off-diagonals in \mathbf{A} and symmetrical, equal-value-diagonals with zero off-diagonals in Σ (Table 2). In fact, all models within 2 AICc units of the best model were OUOU models with zero off-diagonals in Σ and either symmetric, upper, or lower triangular \mathbf{A} matrix models indicating that the primary optima do affect each other (either reciprocally or unidirectionally) and that the trait correlations are caused by these deterministic effects. The first model to include non-zero off-diagonals in Σ was 4.81 AICc units away from the best model but still also includes an \mathbf{A} matrix with non-zero off-diagonals, meaning that if this was the correct model, some of the trait correlations could also be attributed to unmeasured stochastic influences. The first model with diagonal \mathbf{A} and off-diagonal Σ was 8.10 AICc units from the best model; thus, there is far more support for a coevolution model than one that stipulates adaptation to independent primary optima with trait correlations generated by stochastic influences. The rest of the OU models all had far less support, so we do not discuss them further here.

The parameter estimates of the best model can be expressed in terms of Equation 9 as

$$d\mathbf{y}(t) = - \begin{bmatrix} 75 \text{ my}^{-1} & -55 \text{ my}^{-1} \\ -55 \text{ my}^{-1} & 50 \text{ my}^{-1} \end{bmatrix} \left(\mathbf{y}(t) - \begin{bmatrix} 0.53 \text{ mm} \\ 0.82 \text{ mm} \end{bmatrix} \right) dt \\ + \begin{bmatrix} 1.77 \text{ mm}/\sqrt{\text{my}} & 0 \text{ mm}/\sqrt{\text{my}} \\ 0 \text{ mm}/\sqrt{\text{my}} & 1.77 \text{ mm}/\sqrt{\text{my}} \end{bmatrix} d\mathbf{W}(t),$$

where $d\mathbf{y}(t)$ is a 2-dimensional vector consisting of the trait values for the ovipositor length (z_i) in mm of species $i = 1$ to n , and the style length of the specific *Ficus* species the wasps pollinate (x_i) in mm. Similarly, $\mathbf{W}(t)$ is a 2-dimensional standard Wiener process for each trait. Thus, for ovipositor length we can write

$$dz_i = -74.58(z_i - 0.53) + 54.98(x_i - 0.82) + 1.77dW_1,$$

which can be rearranged to give

$$dz_i = -74.58(z_i - 0.53 + 0.74(x_i - 0.82)) + 1.77dW_1,$$

which shows us that ovipositor length follows an Ornstein-Uhlenbeck process with central state, or primary optimum for a fixed value of x_i equal to $0.53 \text{ mm} + 0.74(x_i - 0.82) \text{ mm}$ meaning that the optimum for ovipositor length is a linearly increasing function of style length with a slope of 0.74 (since we used the same units for ovipositor and style length). The optimal ovipositor length, when style length is at its optimum, is 0.53 mm.

We can perform the same operations on the predictive equation for ovipositor length, where, after rewriting and

rearranging:

$$dx_i = -49.63(x_i - 0.82) + 54.98(z_i - 0.53) + 1.77dW_2.$$

We obtain $0.82 \text{ mm} + 1.11(z_i - 0.53) \text{ mm}$. Thus, the optimal style length, when ovipositor length is at its optimum, is 0.82 mm; otherwise, the optimal style length is a linearly increasing function of ovipositor length with a slope of 1.11. We used these equations to generate the expected optimal relationships in Figure 6.

The phylogenetic half-life (1st eigenvalue) for this joint Ornstein-Uhlenbeck process is less than one percent (0.6%) of the tree height, or 44k years. The size of the stochastic fluctuations for ovipositor length, $(1.77)^2/2*75 = 0.02 \text{ mm/my}$ gives the stationary variance of the ovipositor for a fixed style length. Hence the expected distance to the optimum for a fixed style length is $\sqrt{2(0.02)\pi} = 0.11 \text{ mm}$. Note that Σ is a single-value-diagonal matrix, indicative of uncorrelated stochastic evolutionary changes with the same phenotypic rate of change for both variables; thus, the expected distance to the optimum of style length for a fixed ovipositor length is also 0.11 mm. The strong correlation (0.90) between ovipositor and style length associated with this model (Table 2) can be explained in terms of reciprocal selection. In particular, the symmetric \mathbf{A} matrix indicates that the traits influence each other's paths towards their optima.

Interestingly, the worst fitting scenario (BMBM) is the one that reports the lowest correlation between variables (Table 2). This is not surprising considering that, as shown above, the association can be explained by coadaptation, while BMBM can only explain it in terms of correlated stochastic perturbations. Unable to capture the proper evolutionary dynamics, BMBM is most likely underestimating the strength of the association. Also using Brownian motion as the underlying process, Adams & Nason (2018) presented a multivariate permutation-based phylogenetic generalized least squares procedure for testing correlated evolution between traits of coexisting sets of lineages and showcased it with the dataset of Weiblen (2004). Adams & Nason (2018) argued that the high correlation found when ignoring phylogeny (0.90) overestimated the strength of the association between style and ovipositor length given that their method, which accounted for both the plant and pollinator phylogeny in the analysis, reported a much lower correlation (0.55). But if it is true, as our results suggest, that the relationship between ovipositor and style lengths is mediated by selection, the method of Adams & Nason (2018) cannot be expected to fully recover it because its underlying evolutionary process (Brownian motion) is inconsistent with adaptation towards optimal states. Their method

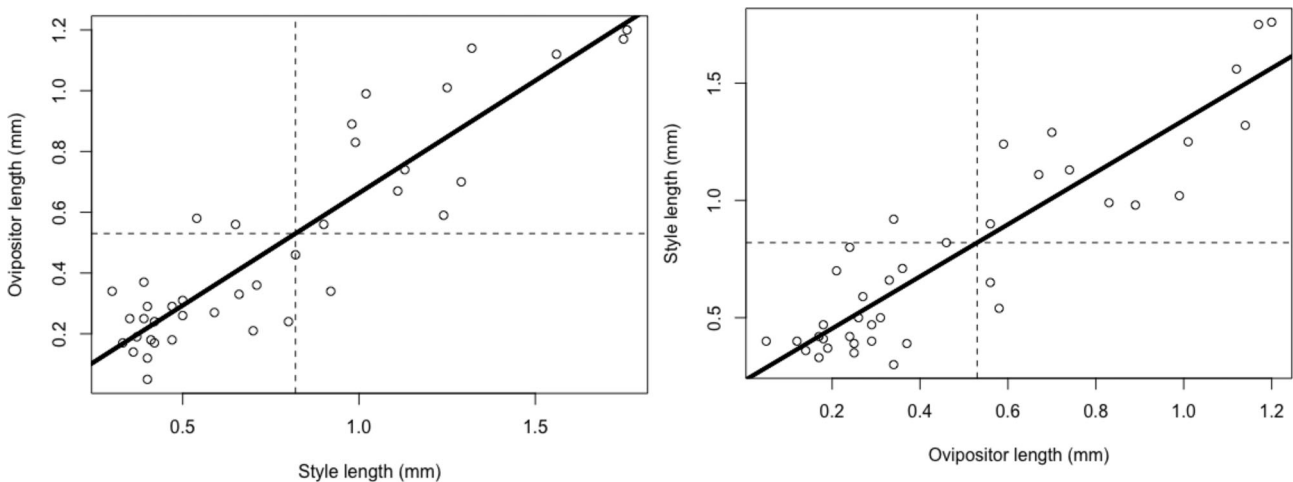


Figure 6. The observed relationship between fig-wasp ovipositor length and fig style length (open circles) with the optimal predictions (see main text) of the multivariate analysis (solid lines). The dashed lines represent where the primary optima for the two traits intersect (i.e., the primary optimum for trait 1 when trait 2 is at its primary optimum). The panel on the left represents the partial regression of ovipositor length on style length, whereas that on the right represents the partial regression of style length on ovipositor length.

is more geared towards evaluating the degree of trait covariation while accounting for the lack of independence between interacting lineages. The problem is that when the dependencies arise from adaptive patterns that are phylogenetically structured (like in the case of interacting lineages that exert selective pressures on each other), such an approach is prone to removing the very same evolutionary patterns that are object of study (Hansen, 2014; Labra et al., 2009). These phylogenetically structured adaptive interactions are quite possible for figs and fig wasps for which highly specialized association precedes the radiation of either lineage, with the fossil record indicating that no major innovations have evolved in this mutualism for at least 34 million years (Compton et al., 2010). From this point of view, it is quite possible that the non-phylogenetic correlation reported by Adams & Nason (2018) did not overestimate the strength of the association between style and ovipositor length (as suggested by the authors) but, like our BMBM here (Table 2), that the phylogenetically corrected correlation was the one underestimating it (in fact, notice that the non-phylogenetic correlation reported by the authors is quite close to the correlations under our Ornstein–Uhlenbeck models, which incorporate phylogenetic information). The approach proposed by Adams & Nason (2018) is valuable in the sense that it allows for testing evolutionary associations involving more than one phylogeny. Coevolution, however, regardless of whether it is specific or diffuse, is most commonly defined by reciprocally mediated selection between interacting species (Nuismer, 2017; Thompson, 2013), and its analysis thus requires analytical approaches that are consistent with selective processes. The adaptation-inertia framework offers the suite of properties required for this task, and some progress has been made in this direction (Drury et al., 2016; Manceau et al., 2017). Still, a more comprehensive approach combining the multivariate Ornstein–Uhlenbeck setup presented above with the simultaneous analysis of several phylogenies as in Adams & Nason (2018) constitutes a promising avenue to rigorously tackle the long-held, but according to Althoff et al. (2014), still untested, assumption that most observed trait variation is a result of coevolutionary processes between ecologically interacting species.

Critical evaluation of the adaptation-inertia framework

Throughout our analysis, we have focused on demonstrating the adaptation-inertia framework, setting aside measurement variance (actual measurement error and within-species variation). This can significantly affect parameter estimates and should be included whenever it is available (unfortunately availability is not always the case, especially for older data sets). For an in-depth discussion, we refer readers to Hansen & Bartoszek (2012) and the forthcoming review of the software for implementing methods of the adaptation-inertia framework (Fuentes-González, in review).

The adaptation-inertia approach and its statistical aspects have undergone critical evaluation Ho and Ané (2014) showed that the accuracy of parameter estimates, particularly for α (rate of adaptation), decreases with smaller α values and that statistical power for α is lower than for other parameters. This emphasizes the need to consider parameter accuracy when drawing conclusions. They also highlighted the presence of ridges in the log-likelihood surface, which can make finding maximum likelihood estimates challenging and lead to non-convergence during optimization. This does not invalidate Ornstein–Uhlenbeck models, but it means conclusions about inertia, stationary variances, and regression parameters require careful consideration of the likelihood surface's topology. Repeating numerical optimizations from different starting points is crucial due to the potential for multiple peaks in parameter-rich models (e.g., Bartoszek et al., 2023a, 2023b).

Cressler et al. (2015) simulated data to identify parameter combinations where the models might break down. They used transformations of the parameters α , θ and σ , to assess their influence on model-selection power. Their findings essentially reiterate observation that α 's magnitude primarily affects the precision and accuracy of its estimate, especially for small sample sizes. Smaller simulation studies (Hansen et al., 2008) also found low estimation precision and accuracy of the α parameter with small α values and few species, but accuracy improves dramatically with larger sample sizes and α values.

Multivariate extensions of the framework have also been critically examined. Adams & Collyer (2018) argued that multivariate phylogenetic comparative methods, including those in the adaptation-inertia framework, (1) become more prone to misidentifying evolutionary processes as trait dimensionality increases and (2) are prone to rotation invariance issues in that the likelihood of a given model can change after orthogonal linear transformation of its variables. Bartoszek et al., (2023b) provide a comprehensive treatment of how these issues arise and how they can be alleviated and even used to our advantage. The first issue is due to the traditional practice of explicitly constructing the whole among-species–among-trait variance matrix V and then calculating the likelihood directly from the multivariate normal density. In practice, V is often ill-conditioned, which leads to substantial numerical errors and potential likelihood biases towards more complex models. This issue is alleviated by Mitov et al.’s (2020) fast-likelihood calculation algorithm, implemented in the PCMBASE package, which performs calculations branch by branch rather than on the entire V matrix. The latest versions of packages such as mvSLOUCH (Bartoszek, 2024) use PCMBASE as their computational engines. Furthermore, the significantly faster calculations allow for many more iterations of numerical optimizers on large phylogenies. These improvements together lead to more stable likelihood estimates, substantially alleviating the potential bias towards more complex models. The rotation invariance issue is more convoluted and is related to likelihood instability rather than true rotation invariance and is potentially an issue with any method that uses numerical rather than analytical optimization procedures. Bartoszek et al., (2023b), however, argue that the different likelihoods achieved by different rotations of the data could be used to our advantage in that they could be used to determine model convergence as well as to ease estimation as some rotations may lead to more independent data points than others.

Future directions

Modelling trait evolution on a dynamical adaptive landscape is one of the great strengths of the adaptation-inertia approach. Hundreds of studies have implemented the methods of the adaptation-inertia framework on traits ranging from brain volume to gene expression. A quantitative meta-analysis of these and future studies to determine (a) how often adaptive hypotheses provide the best explanation for trait change; (b) how fast adaptation occurs, and (c) what the relative contributions of adaptive versus stochastic change are would be highly informative. Unfortunately, relevant parameters from the fitted Ornstein–Uhlenbeck models, or tree heights, or measurement error are sporadically reported, which lowers the power of the suggested meta-analysis. We therefore encourage future users of the adaptation-inertia approach to always report all model parameters, at least as supplements if space requirements prohibit this, with units and their confidence estimates so that the barriers to informative meta-analysis might be alleviated.

One challenge with the adaptation-inertia approach is that the model parameters are somewhat open for interpretation compared to stricter microevolutionary interpretations when describing trait dynamics in a static landscape (e.g., Lande, 1976). Whereas a phylogenetic comparative study of young populations that have diversified over a few thousand years may allow for interpreting the Ornstein–Uhlenbeck process

parameters in line with quantitative genetic models, rather than in the more-vague “macroevolutionary” terms, most across-species comparative data span many millions of years. Analyzing comparative data covering different timescales and assessing when the microevolutionary interpretation of the model parameters breaks down could add insight into how to connect microevolutionary processes with the larger-scale patterns of phenotypic evolution observed at macroevolutionary timescales.

“Chicken or egg” type questions abound when it comes to inferring patterns of transitional evolutionary changes, and the phylogenetic comparative methods we have described can contribute to such inference. Consider the study of Davis et al. (2012), which concerns the evolution of egg and body size in geometrid moths. The two traits are strongly correlated across species, and the question of whether increasing body size drives larger egg size or whether it is the other way around arose. The following logic was used to infer which trait drives the relationship: first an Ornstein–Uhlenbeck model with no predictor variables was fit for each trait independently, which, as discussed above, is a way to quantify the degree of phylogenetic signal in a trait (captured by the phylogenetic half-life). Then each trait was modelled on optima regressed on the other trait to determine which model exhibited the highest degree of phylogenetic inertia (again measured by the phylogenetic half-life). Using this approach, we are essentially asking (as in Labra et al., 2009) if the phylogenetic signal observed in a trait is due to inertia in evolution of the trait itself or whether it is rapidly tracking another variable or trait that is phylogenetically structured. For Davis et al. (2012), strong phylogenetic signal was observed in egg size, but when regressed on body size, a significant regression with almost no phylogenetic inertia was observed. For body size, both strong phylogenetic signal and phylogenetic inertia were observed, despite the strong regression relationship. From these observations, we can conclude that the strong correlation between the traits exists because egg size is likely tracking changes in body size rather than vice versa. This logic has further been used to infer which life history traits in passerines are the likely drivers of evolutionary change (Pienaar et al., 2013), although see Uyeda et al. (2015) for a relevant critique of dimensional reduction prior to the use of phylogenetic comparative methodologies. The multivariate, generalized Ornstein–Uhlenbeck framework (Bartoszek et al., 2012) uses more refined logic to make inferences regarding which traits are driving an observed relationship and suggests that inference is not as straight forward as argued above. The ability to estimate generalized non-symmetrical A matrices that include off-diagonal elements allow us to infer to what degree traits influence each other’s evolution and potentially which traits are driving observed correlations. For models where two or more traits are evolving as a multivariate Ornstein–Uhlenbeck process, the estimated parameters, along with the A matrix associated eigenvectors and eigenvalues, allow for inferences regarding which variables influence each other. García-Cabello et al. (2022) recently used this logic to infer that the evolution of superfetation precedes the evolution of advanced placentotrophy in poecilid fish.

The existing multivariate formulations of the adaptation-inertia framework allow for testing hypotheses that involve comparison of trait interactions within individuals, such as evolutionary trade-offs. The ability to analyze adaptive trait interactions between two or more unrelated sets of lineages,

such as those that occur between coevolving lineages, would provide an invaluable tool for biodiversity researchers and, we argue, could also potentially explain some of the phenomena observed in macroevolutionary data, such as the commonly observed pervasive trait fluctuations around a fixed mean punctuated with burst of change (Uyeda et al., 2011). Furthermore, most phylogenetic comparative methods use bifurcating trees to inform their residual covariance structures. The reticulate nature of many, if not most, species trees due to hybridization or horizontal gene transfer is becoming ever more apparent—the continued development of methods to incorporate such reticulations, such as network structures (Bastide et al., 2018), in our opinion, will likely also inform methods to study more widespread diffuse coevolution in a phylogenetic comparative framework and are thus well worth pursuing.

Supplementary material

Supplementary material is available at *Journal of Evolutionary Biology* online.

Data availability

The data underlying this article has been published elsewhere and can be obtained on Dryad. <https://doi.org/10.5061/dryad.r3765>.

Author contributions

Jason Pienaar (Conceptualization [lead], Data curation [lead], Formal Analysis [lead], Funding acquisition [lead], Investigation [lead], Methodology [lead], Project administration [lead], Software [equal], Supervision [equal], Validation [lead], Visualization [lead], Writing – original draft [lead], Writing – review & editing [lead]), Krzysztof Bartoszek (Conceptualization [equal], Methodology [equal], Software [equal], Writing – review & editing [equal]), Bayu Brahmantio (Formal Analysis [supporting], Software [supporting], Visualization [supporting]), Janna L. Fierst (Conceptualization [equal], Visualization [equal], Writing – review & editing [equal]), Jesualdo A. Fuentes-González (Conceptualization [equal], Data curation [supporting], Formal Analysis [supporting], Investigation [supporting], Methodology [supporting], Software [supporting], Visualization [supporting], Writing – review & editing [equal]), Thomas F. Hansen (Conceptualization [equal], Methodology [supporting], Software [supporting], Writing – review & editing [equal]), Woodrow Hao C. Kiang (Formal Analysis [supporting], Software [supporting], Visualization [supporting]), Bjørn T. Kopperud (Software [equal], Writing – review & editing [equal]), and Kjetil L. Voje (Methodology [supporting], Software [supporting], Writing – review & editing [equal])

Funding

For J.P., this material is based upon work supported by the National Science Foundation under grant numbers 2225683 and 2412309. For J.F., this material is based upon work supported by the National Science Foundation under grant numbers 2045035 and 1941854. K.B. is supported by a Swedish Research Council (Vetenskapsrådet) grant no. 2017-0495 and an ELLIIT Call C grant, the former also supports H.C.K.,

and the latter supports B.B. K.L.V. is supported by an European Research Council-2020-STG (Grant agreement ID: 948465). B.T.K. was supported by the Deutsche Forschungsgemeinschaft (DFG) Emmy Noether Program (Award HO 6201/1-1) and by an European Research Council MacDrive, GA 101043187).

Conflicts of interest

None declared.

References

Adams, D. C., & Collyer, M. L. (2018). Multivariate phylogenetic comparative methods: Evaluations, comparisons, and recommendations. *Systematic Biology*, 67(1), 14–31. <https://doi.org/10.1093/sysbio/syx055>

Althoff, D. M., Segraves, K. A., & Johnson, M. T. J. (2014). Testing for coevolutionary diversification: linking pattern with process. *Trends in Ecology & Evolution*, 29, 82–89. <https://doi.org/10.1016/j.tree.2013.11.003>

Armbruster, W. S. (1988). Multilevel comparative analysis of the morphology, function, and evolution of dalechampia blossoms: Ecological archives E069-002. *Ecology*, 69(6), 1746–1761. <https://doi.org/10.2307/1941153>

Armbruster, W. S., Pélabon, C., Bolstad, G. H., & Hansen, T. F. (2014). Integrated phenotypes: Understanding trait covariation in plants and animals. *Philosophical Transactions of the Royal Society B: Biological Sciences*, 369(1649), 20130245. <https://doi.org/10.1093/rstb.2013.0245>

Arnold, S. J. (2023). *Evolutionary quantitative genetics*. Oxford University Press. <https://doi.org/10.1093/oso/9780192859389.001.0001>

Arnold, S. J., Pfrender, M. E., & Jones, A. G. (2001). The adaptive landscape as a conceptual bridge between micro- and macroevolution. *Genetica*, 112–113, 9–32. <https://doi.org/10.1023/A:1013373907708>

Bartoszek, K., Fuentes-González, J. A., Mitov, V., ... Voje, K. L. (2023a). Model Selection Performance in Phylogenetic Comparative Methods Under Multivariate Ornstein–Uhlenbeck Models of Trait Evolution. *Systematic Biology*, 72, 275–293. <https://doi.org/10.1093/sysbio/syac079>

Bartoszek, K., Fuentes-González, J. A., Mitov, V., ... Voje, K. L. (2023b). Analytical advances alleviate model misspecification in non-Brownian multivariate comparative methods. *Evolution*, 78, 389–400. <https://doi.org/10.1093/evolut/qpad185>

Bartoszek, K., Pienaar, J., Mostad, P., ... Hansen, T. F. (2012). A phylogenetic comparative method for studying multivariate adaptation. *Journal of Theoretical Biology*, 314, 204–215. <https://doi.org/10.1016/j.jtbi.2012.08.005>

Bartoszek, K., Tredgett Clarke, J., Fuentes-González, J., ... Voje, K. L. (2024). Fast mvSLOUCH: Multivariate Ornstein–Uhlenbeck-based models of trait evolution on large phylogenies. *Methods in Ecology and Evolution*, 15, 1507–1515. <https://doi.org/10.1111/2041-210X.14376>

Bastide, P., Ané, C., Robin, S., & Mariadassou, M. (2018). Inference of adaptive shifts for multivariate correlated traits. *Systematic Biology*, 67(4), 662–680. <https://doi.org/10.1093/sysbio/syy005>

Bastide, P., Mariadassou, M., & Robin, S. (2017). Detection of adaptive shifts on phylogenies by using shifted stochastic processes on a tree. *Journal of the Royal Statistical Society Series B: Statistical Methodology*, 79(4), 1067–1093. <https://doi.org/10.1111/rssb.12206>

Beaulieu, J.M., Jhwueng, DC., Boettiger, C., & O’Meara, BC. (2012). Modeling stabilizing selection: expanding the Ornstein–Uhlenbeck model of adaptive evolution. *Evolution*, 66, 2369–83. <https://doi.org/10.1111/j.1558-5646.2012.01619.x>

Beaulieu, J. M., & O'Meara, B. C. (2016). Detecting Hidden Diversification Shifts in Models of Trait-Dependent Speciation and Extinction. *Systematic Biology*, 65, 583–601. <https://doi.org/10.1093/sysbio/syw022>

Beaulieu, J., & O'Meara, B. (2025). OUwie: Analysis of evolutionary rates in an OU framework (R package). <https://github.com/thej022/214/OUwie>. Date accessed October 14, 2025.

Boyko, J. D., O'Meara, B. C., & Beaulieu, J. M. (2023). A novel method for jointly modeling the evolution of discrete and continuous traits. *Evolution*, 77(3), 836–851. <https://doi.org/10.1093/evolut/qpad002>

Bradshaw, A. D. (1991). The Croonian Lecture, 1991: Genostasis and the limits to evolution. *Philosophical Transactions: Biological Sciences*, 333(1267), 289–305.

Brooks, D. R., & McLennan, D. A. (1991). *Phylogeny, ecology, and behavior: a research program in comparative biology*. University of Chicago press.

Burnham, K. P., & Anderson, D. R. (1998). Practical use of the information-theoretic approach. In *Model selection and inference* (pp. 75–117). Springer. <https://doi.org/10.1007/978-1-4757-2917-7>

Burnham, K. P., & Anderson, D. R. (2004). Multimodel inference: Understanding AIC and BIC in model selection. *Sociological Methods & Research*, 33(2), 261–304. <https://doi.org/10.1177/0049124104268644>

Burt, A. (1989). Comparative methods using phylogenetically independent contrasts. *Oxford Surveys in Evolutionary Biology*, 6, 33–53.

Butler, M. A., & King, A. A. (2004). Phylogenetic comparative analysis: A modeling approach for adaptive evolution. *The American Naturalist*, 164(6), 683–695. <https://doi.org/10.1086/426002>

Calsbeck, R., Gosden, T. P., Kuchta, S. R., & Svensson, E. I. (2012). Fluctuating selection and dynamic adaptive landscapes. *The Adaptive Landscape in Evolutionary Biology*, 23, 89–109.

Catalán, A., Briscoe, A. D., & Höhna, S. (2019). Drift and directional selection are the evolutionary forces driving gene expression divergence in eye and brain tissue of *Heliconius* butterflies. *Genetics*, 213(2), 581–594. <https://doi.org/10.1534/genetics.119.02493>

Cheverud, J. M., Dow, M. M., & Leutenegger, W. (1985). The quantitative assessment of phylogenetic constraints in comparative analyses—Sexual dimorphism in body-weight among primates. *Evolution*, 39(6), 1335–1351. <https://doi.org/10.2307/2408790>

Clavel, J., Escarguel, G., & Merceron, G. (2015). mvMORPH: An R package for fitting multivariate evolutionary models to morphometric data. *Methods in Ecology and Evolution*, 6(11), 1311–1319. <https://doi.org/10.1111/2041-210X.12420>

Compton, S. G., Ball, A. D., Collinson, M. E., ... Ross, A. J. (2010). Ancient fig wasps indicate at least 34 Myr of stasis in their mutualism with fig trees. *Biology letters*, 6, 838–842. <https://doi.org/10.1098/rsbl.2010.0389>

Cressler, C. E., Butler, M. A., & King, A. A. (2015). Detecting adaptive evolution in phylogenetic comparative analysis using the Ornstein-Uhlenbeck model. *Systematic Biology*, 64(6), 953–968. <https://doi.org/10.1093/sysbio/syv043>

Cruaud, A., Rønsted, N., Chantarasuwan, B., ... Savolainen, V. (2012). An extreme case of plant-insect codiversification: Figs and fig-pollinating wasps. *Systematic Biology*, 61(6), 1029–1047. <https://doi.org/10.1093/sysbio/sys068>

Davis, R. B., Javoviš, J., Pienaar, J., ... Tammaru, T. (2012). Disentangling determinants of egg size in the Geometridae (Lepidoptera) using an advanced phylogenetic comparative method. *Journal of Evolutionary Biology*, 25(1), 210–219. <https://doi.org/10.1111/j.1420-9101.2011.02420.x>

Deaner, R. O., & Nunn, C. L. (1999). How quickly do brains catch up with bodies? A comparative method for detecting evolutionary lag. *Proceedings of the Royal Society of London. Series B: Biological Sciences*, 266(1420), 687–694. <https://doi.org/10.1098/rspb.1999.0690>

Dobzhansky, T. (1937). Genetic nature of species differences. *The American Naturalist*, 71, 404–420. <https://doi.org/10.1086/280726>

Drury, J., Clavel, J., Manceau, M., & Morlon, H. (2016). Estimating the effect of competition on trait evolution using maximum likelihood inference. *Systematic Biology*, 65, 700–710. <https://doi.org/10.1093/sysbio/syv020>

Eldredge, N., & Gould, S. J. (1972). Punctuated equilibria: An alternative to phyletic gradualism. In T. J. M. Schopf (Ed.), *Models in paleobiology* (pp. 82–115). Freeman, Cooper.

Felsenstein, J. (1985). Phylogenies and the comparative method. *The American Naturalist*, 125(1), 1–15. <https://doi.org/10.1086/284325>

Felsenstein, J. (1988). Phylogenies and quantitative characters. *Annual Review of Ecology and Systematics*, 19, 445–471. <https://doi.org/10.1146/annurev.es.19.110188.002305>

Futuyma, D. J. (2010). Evolutionary constraint and ecological consequences. *Evolution*, 64(7), 1865–1884. <https://doi.org/10.1111/j.1558-5646.2010.00960.x>

Futuyma, D. J., & Kirkpatrick, M. (2023). *Evolution*. (Fifth edn). Oxford University Press.

Garcia-Cabello, K. N., Fuentes-Gonzalez, J. A., Saleh-Subaie, N., ... Zuniga-Vega, J. J. (2022). Increased superfetation precedes the evolution of advanced degrees of placentotrophy in viviparous fishes of the family Poeciliidae. *Biology Letters*, 18(10), 20220173. <https://doi.org/10.1098/rsbl.2022.0173>

Grabowski, M., Kopperud, B. T., Tsuboi, M., & Hansen, T. F. (2023). Both diet and sociality affect primate brain-size evolution. *Systematic Biology*, 72(2), 404–418. <https://doi.org/10.1093/sysbio/syac075>

Grabowski, M., Vojte, K. L., & Hansen, T. F. (2016). Evolutionary modeling and correcting for observation error support a 3/5 brain-body allometry for primates. *Journal of human evolution*, 94, 106–116. <https://doi.org/10.1016/j.jhevol.2016.03.001>

Grafen, A. (1989). The phylogenetic regression. *Philosophical Transactions of the Royal Society of London. B, Biological Sciences*, 326(1233), 119–157. <https://doi.org/10.1098/rstb.1989.0106>

Hadfield, J. D. (2010). MCMC methods for multi-response generalized linear mixed models: The MCMCglmm R package. *Journal of Statistical Software*, 33(2), 1–22. <https://doi.org/10.18637/jss.v033.i02>

Hansen, T. F. (1997). Stabilizing selection and the comparative analysis of adaptation. *Evolution*, 51(5), 1341–1351. <https://doi.org/10.2307/2411186>

Hansen, T. F. (2012). Adaptive landscapes and macroevolutionary dynamics. In *The adaptive landscape in evolutionary biology* (Vol. 205, p. 26). Oxford University Press. <https://doi.org/10.1093/acprof:oso/9780199595372.003.0013>

Hansen, T. F. (2014). Use and misuse of comparative methods in the study of adaptation. In L. Z. Garamszegi (Ed.), *Modern phylogenetic comparative methods and their application in evolutionary biology* (pp. 351–379). Springer. https://doi.org/10.1007/978-3-662-43550-2_14

Hansen, T. F. (2024). Three modes of evolution? Remarks on rates of evolution and time scaling. *Journal of Evolutionary Biology*, 37(12), 1523–1537. <https://doi.org/10.1093/jeb/voae071>

Hansen, T. F., & Bartoszek, K. (2012). Interpreting the evolutionary regression: The interplay between observational and biological errors in phylogenetic comparative studies. *Systematic Biology*, 61(3), 413–425. <https://doi.org/10.1093/sysbio/syr122>

Hansen, T. F., & Houle, D. (2004). Evolvability, stabilizing selection, and the problem of stasis. In M. Pigliucci, & K. Preston (Eds.), *Phenotypic integration: studying the ecology and evolution of complex phenotypes* (pp. 130–150). Oxford University Press. <https://doi.org/10.1093/oso/9780195160437.001.0001>

Hansen, T. F., & Martins, E. P. (1996). Translating between microevolutionary process and macroevolutionary patterns: The correlation structure of interspecific data. *Evolution*, 50(4), 1404–1417. <https://doi.org/10.2307/2410878>

Hansen, T. F., & Orzack, S. H. (2005). Assessing current adaptation and phylogenetic inertia as explanations of trait evolution: The need for controlled comparisons. *Evolution*, 59(10), 2063–2072. <https://doi.org/10.1111/j.0014-3820.2005.tb00917.x>

Hansen, T. F., & Pélabon, C. (2021). Evolvability: A quantitative-genetics perspective. *Annual Review of Ecology, Evolution, and Systematics*, 52(1), 153–175. <https://doi.org/10.1146/annurev-ecolsys-011121-021241>

Hansen, T. F., Pienaar, J., & Orzack, S. H. (2008). A comparative method for studying adaptation to a randomly evolving environment. *Evolution: International Journal of Organic Evolution*, 62(8), 1965–1977. <https://doi.org/10.1111/j.1558-5646.2008.00412.x>

Hipp, A. L., & Escudero, M. (2010). MATICCE: Mapping transitions in continuous character evolution. *Bioinformatics*, 26(1), 132–133. <https://doi.org/10.1093/bioinformatics/btp625>

Ho, L. S. T., & Ané, C. (2014). A Linear-Time Algorithm for Gaussian and Non-Gaussian Trait Evolution Models. *Systematic Biology*, 63(3) 397–408. <https://doi.org/10.1093/sysbio/syu005>

Holstad, A., Voje, K. L., Opedal, Ø. H., ... Pélabon, C. (2024). Evolvability predicts macroevolution under fluctuating selection. *Science*, 384(6696), 688–693. <https://doi.org/10.1126/science.ad18722>

Hunt, G. (2006). Fitting and comparing models of phyletic evolution: random walks and beyond. *Paleobiology*, 32, 578–601.

Hunt, G. (2007). The relative importance of directional change, random walks, and stasis in the evolution of fossil lineages. *Proceedings of the National Academy of Sciences*, 104, 18404–18408. <https://doi.org/10.1073/pnas.0704088104>

Hunt, G. (2008). Gradual or pulsed evolution: When should punctuational explanations be preferred? *Paleobiology*, 34(3), 360–377. <https://doi.org/10.1666/07073.1>

Hunt, G., Hopkins, M. J., & Lidgard, S. (2015). Simple versus complex models of trait evolution and stasis as a response to environmental change. *Proceedings of the National Academy of Sciences*, 112(16), 4885–4890. <https://doi.org/10.1073/pnas.1403662111>

Hurvich, C. M., & Tsai, C.-L. (1989). Regression and time series model selection in small samples. *Biometrika*, 76(2), 297–307. <https://doi.org/10.1093/biomet/76.2.297>

Ingram, T., & Mahler, D. L. (2013). SURFACE: Detecting convergent evolution from comparative data by fitting Ornstein–Uhlenbeck models with stepwise AIC. *Methods in Ecology and Evolution*, 4(5), 416–425. <https://doi.org/10.1111/2041-210X.12034>

Ives, A. R., & Garland Jr, T. (2010). Phylogenetic logistic regression for binary dependent variables. *Systematic Biology*, 59(1), 9–26. <https://doi.org/10.1093/sysbio/syp074>

Ives, A. R., & Garland Jr, T. (2014). Phylogenetic regression for binary dependent variables. In *Modern phylogenetic comparative methods and their application in evolutionary biology* (pp. 231–261). Springer. <https://doi.org/10.1007/978-3-662-43550-2>

Kemp, T. (1982). *Mammal-like reptiles and the origin of mammals*. Academic Pr.

Kemp, T. (2006). The origin and early radiation of the therapsid mammal-like reptiles: A palaeobiological hypothesis. *Journal of Evolutionary Biology*, 19(4), 1231–1247. <https://doi.org/10.1111/j.1420-9101.2005.01076.x>

Kemp, T. (2007). The concept of correlated progression as the basis of a model for the evolutionary origin of major new taxa. *Proceedings of the Royal Society B: Biological Sciences*, 274(1618), 1667–1673. <https://doi.org/10.1098/rspb.2007.0288>

Khabbazian, M., Kriebel, R., Rohe, K., & Ané, C. (2016). Fast and accurate detection of evolutionary shifts in Ornstein–Uhlenbeck models. *Methods in Ecology and Evolution*, 7(7), 811–824. <https://doi.org/10.1111/2041-210x.12534>

King, A. A., & Butler, M. A. (2009). Ouch: Ornstein–Uhlenbeck models for phylogenetic comparative hypotheses, version 2.9-2 (R package). <http://r-forge.r-project.org/ouch/>. Date accessed October 15, 2025.

Kopperud, B. T., Pienaar, J., Voje, K. L., ... Grabowski, M. (2020). Slouch: Stochastic Linear Ornstein–Uhlenbeck Comparative Hypotheses. R package version 2.1.4. <https://github.com/kopperud/slouch>. Date accessed October 15, 2025.

Labra, A., Pienaar, J., & Hansen, T. F. (2009). Evolution of thermal physiology in Liolaemus lizards: Adaptation, phylogenetic inertia, and niche tracking. *The American Naturalist*, 174(2), 204–220. <https://doi.org/10.1086/600088>

Lajeunesse, M. J. (2009). Meta-analysis and the comparative phylogenetic method. *The American Naturalist*, 174(3), 369–381. <https://doi.org/10.1086/603628>

Lajeunesse, M. J. (2011). phyloMeta: A program for phylogenetic comparative analyses with meta-analysis. *Bioinformatics*, 27(18), 2603–2604. <https://doi.org/10.1093/bioinformatics/btr438>

Lande, R. (1976). Natural-selection and random genetic drift in phenotypic evolution. *Evolution*, 30(2), 314–334. <https://doi.org/10.1111/j.1558-5646.1976.tb00911.x>

Latrille, T., Julien, J., Hartasánchez, D. A., & Salamin, N. (2024). Estimating the proportion of beneficial mutations that are not adaptive in mammals. *PLOS Genetics*, 20(12), e1011536. <https://doi.org/10.1371/journal.pgen.1011536>

Lynch, M. (1991). Methods for the analysis of comparative data in evolutionary biology. *Evolution*, 45(5), 1065–1080. <https://doi.org/10.2307/2409716>

Manceau, M., Lambert, A., & Morlon, H. (2017). A unifying comparative phylogenetic framework including traits coevolving across interacting lineages. *Systematic biology*, 66, 551–568.

Martin, R. D., & Harvey, P. H. (1985). Brain size allometry ontogeny and phylogeny. In *Size and scaling in primate biology* (pp. 147–173). Springer. <https://doi.org/10.1007/978-1-4899-3647-9>

Martins, E. P. (2000). Adaptation and the comparative method. *Trends in Ecology & Evolution*, 15(7), 296–299. [https://doi.org/10.1016/S0169-5347\(00\)01880-2](https://doi.org/10.1016/S0169-5347(00)01880-2)

Martins, E. P., & Hansen, T. F. (1997). Phylogenies and the comparative method: A general approach to incorporating phylogenetic information into the analysis of interspecific data. *The American Naturalist*, 149(4), 646–667. <https://doi.org/10.1086/286013>

May, M. R., & Moore, B. R. (2020). A Bayesian approach for inferring the impact of a discrete character on rates of continuous-character evolution in the presence of background-rate variation. *Systematic Biology*, 69(3), 530–544. <https://doi.org/10.1093/sysbio/syz069>

Mitov, V., Bartoszek, K., Asimomitis, G., & Stadler, T. (2020). Fast likelihood calculation for multivariate Gaussian phylogenetic models with shifts. *Theoretical Population Biology*, 131, 66–78.

Mitov, V., Bartoszek, K., & Stadler, T. (2019). Automatic generation of evolutionary hypotheses using mixed Gaussian phylogenetic models. *Proceedings of the National Academy of Sciences*, 116(34), 16921–16926. <https://doi.org/10.1073/pnas.1813823116>

Moen, D. S., Morlon, H., & Wiens, J. J. (2016). Testing convergence versus history: Convergence dominates phenotypic evolution for over 150 million years in frogs. *Systematic Biology*, 65(1), 146–160. <https://doi.org/10.1093/sysbio/syv073>

Nefdt, R. J. C., & Compton, S. G. (1996). Regulation of seed and pollinator production in the fig–fig wasp mutualism. *The Journal of Animal Ecology*, 65(2), 170. <https://doi.org/10.2307/5720>

Nuismer, S. (2017). *Introduction to coevolutionary theory*. Macmillan Higher Education. 9781319129811

Pagel, M. D., & Harvey, P. H. (1988). Recent developments in the analysis of comparative data. *The Quarterly Review of Biology*, 63(4), 413–440. <https://doi.org/10.1086/416027>

Pienaar, J., Ilany, A., Geffen, E., & Yom-Tov, Y. (2013). Macroevolution of life-history traits in passerine birds: Adaptation and phylogenetic inertia. *Ecology Letters*, 16(5), 571–576. <https://doi.org/10.1111/ele.12077>

Posada, D., & Buckley, T. R. (2004). Model selection and model averaging in phylogenetics: Advantages of Akaike information criterion and Bayesian approaches over likelihood ratio tests. *Systematic Biology*, 53(5), 793–808. <https://doi.org/10.1080/10635150490522304>

Reitan, T., Schweder, T., & Henderiks, J. (2012). Phenotypic evolution studied by layered stochastic differential equations. *The Annals of Applied Statistics*, 6(4), 1531–1551. <https://doi.org/10.1214/12-AOAS559>

Rensch, B. (1959). *Evolution above the species Level*. Columbia University Press. <https://doi.org/10.7312/rens91062>

Revell, L. J. (2010). Phylogenetic signal and linear regression on species data: *Phylogenetic regression. Methods in Ecology and Evolution*, 1(4), 319–329. <https://doi.org/10.1111/j.2041-210X.2010.00044.x>

Ridley, M. (1983). *The explanation of organic diversity: the comparative method and adaptations for mating*. Clarendon.

Rohlf, F. J. (2001). Comparative methods for the analysis of continuous variables: Geometric interpretations. *Evolution*, 55(11), 2143–2160.

Simpson, G. G. (1944). *Tempo and mode in evolution*, (Issue 15). Columbia University Press.

Simpson, G. G. (1953). *The major features of evolution*. Columbia University Press. <https://doi.org/10.7312/simp93764>

Thompson, J. N. (2013). *Relentless evolution*. University of Chicago Press.

Tibshirani, R. (1996). Regression shrinkage and selection via the lasso. *Journal of the Royal Statistical Society Series B: Statistical Methodology*, 58(1), 267–288. <https://doi.org/10.1111/j.2517-6161.1996.tb02080.x>

Uyeda, J. C., Caetano, D. S., & Pennell, M. W. (2015). Comparative analysis of principal components can be misleading. *Systematic Biology*, 64(4), 677–689. <https://doi.org/10.1093/sysbio/syv019>

Uyeda, J. C., & Harmon, L. J. (2014) A novel Bayesian method for inferring and interpreting the dynamics of adaptive landscapes from phylogenetic comparative data. *Systematic Biology*, 63(6), 902–918. <https://doi.org/10.1093/sysbio/syu057>

Uyeda, J. C., Hansen, T. F., Arnold, S. J., & Pienaar, J. (2011). The million-year wait for macroevolutionary bursts. *Proceedings of the National Academy of Sciences*, 108(38), 15908–15913. <https://doi.org/10.1073/pnas.1014503108>

Uyeda, J. C., Zenil-Ferguson, R., & Pennell, M. W. (2018) Rethinking phylogenetic comparative methods. *Systematic Biology*, 67, 1091–1109. <https://doi.org/10.1093/sysbio/syy031>

Voje, K. L. (2016). Tempo does not correlate with mode in the fossil record. *Evolution*, 70(12), 2678–2689. <https://doi.org/10.1111/evo.13090>

Voje, K. L. (2020). Testing eco-evolutionary predictions using fossil data: Phyletic evolution following ecological opportunity. *Evolution*, 74, 188–200. <https://doi.org/10.1111/evo.13838>

Voje, K. L. (2023). Fitting and evaluating univariate and multivariate models of within-lineage evolution. *Paleobiology*, 49(4), 747–764. <https://doi.org/10.1017/pab.2023.10>

Weinblen, G. D. (2004). Correlated evolution in fig pollination. *Systematic Biology*, 53(1), 128–139. <https://doi.org/10.1080/10635150490265012>

Williams, G. C. (1992). *Natural selection: domains, levels, and challenges*. Oxford Univ. Press. <https://doi.org/10.1093/oso/9780195069327.001.0001>

Wright, S. (1931). Evolution in mendelian populations. *Genetics*, 16, 97–159. <https://doi.org/10.1093/genetics/16.2.97>